Development of Improved Loop Joint Applied for Precast PC Deck Slab

Hatakeyama, Shigetada
Civil Engineering Division, Fuji P.S Corporation : Engineer

Sagawa, Yasutaka
九州大学大学院工学研究院社会基盤部門 : 准教授

Hamada, Hidenori
Department of Civil and Structural Engineering, Kyushu University : Professor

Hino, Shinichi
National Institute of Technology, Oita College : Principal

他

https://hdl.handle.net/2324/4481588

出版情報：Journal of Advanced Concrete Technology. 19 (6), pp.644-654, 2021-06-17. 日本コンクリート工学会
バージョン：

Technical report

Development of Improved Loop Joint Applied for Precast PC Deck Slab

Shigetada Hatakeyama[1*], Yasutaka Sagawa[2], Hidenori Hamada[3], Shinichi Hino[4], Mamoru Masaki[5] and Yuji Sato[6]

Received 30 December 2020, accepted 7 June 2021 doi:10.3151/jact.19.644

Abstract

Ordinary "loop joint" applied to precast prestressed concrete (PC) deck slab tends to increase its thickness. By decreasing this thickness, the dead load of the deck slab can be reduced. Hence, we have developed an "improved (inclined) loop joint" that reduces the deck slab thickness. This study presents the results of static bending test of slab specimens to confirm the load-carrying behavior and wheel moving load test to examine the fatigue durability of precast PC deck slabs with improved loop joints.

The bending load-carrying behavior satisfied the requirements for highways in Japan. In addition, in the wheel moving load test, no sudden increase in vertical deflection and joint opening was confirmed at a load step of 250 kN × 100 000 times equivalent to 100 years on an actual bridge. Moreover, there was no water leakage at the bottom surface of the deck slab during the water-filling test. Based on the test results, it was inferred that the required load-carrying behavior and fatigue durability could be retained for 100 years in the improved loop joint.

1. Introduction

In Japan, renewal projects for the reconstruction of heavily deteriorated road structures are underway, especially for highways. The replacement of deck slab of the road bridges is the primary work of the renewal projects, and precast PC deck slabs with high durability are often used. According to the outline of bridge specifications (NEXCO 2017), the thickness of precast PC deck slabs using loop connection is 220 mm when the span of each main girder is up to 3.6 m in the plate girder-type bridge. However, owing to the rank up of the loop rebar diameter caused by the negative bending moment near the intermediate support point or due to the change in the cross slope, the total thickness of the deck slab increases followed by an increase in the dead load. The increase in deck thickness is restricted by the bending diameter of the loop reinforcing bar. If the diameter of the reinforcing bar is increased, then its minimum bending diameter also increases, thus increasing the deck thickness. Reducing the weight of the slab is very important to ensure the load-bearing capacity of the existing steel girders and seismic resistance of the bridge; hence, it is necessary to reduce the thickness of the slab.

Extensive research on the loop joint system has been conducted to study the characteristics and features of the joints to enhance the effectiveness of precast decks not only in Japan but also in other countries (Ryu *et al*. 2007; Henrik and Linh 2013). However, research on tilted loop joints except for horizontal loop connections (Ong *et al*. 2006) is rather limited.

To solve this technical problem, we developed an "improved (inclined) loop joint" to reduce the thickness of the deck slab with the loop joint, which has abundant achievements and high reliability. **Figure 1** shows the improved loop joint, and **Fig. 2** shows a comparison of the ordinary and improved loop joints. The loop reinforcing bar is inclined in the transverse direction such that the slab thickness can be reduced while maintaining the minimum bending radius of the loop reinforcing bars.

This study presents the experimental results of the static loading test and wheel moving load test for a tilted loop connection. The former analyzes the bending load-carrying performance of the RC beam while the latter analyzes the fatigue durability of the precast PC slab.

Part of this paper contains the English translation from the authors' previous work (Hatakeyama *et al*. 2018a,

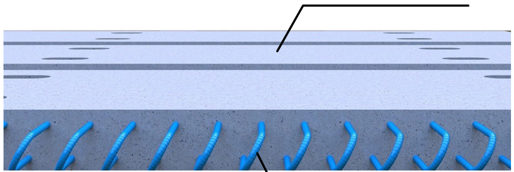

Fig. 1 The image figure of improved loop joint.

[1]Engineer, Civil Engineering Division, Fuji P.S Corporation, Fukuoka, Japan. *Corresponding author, *E-mail*: s.hatakeyama@fujips.co.jp
[2]Associate Professor, Dept. of Civil and Structural Engineering, Kyushu University, Fukuoka, Japan.
[3]Professor, Dept. of Civil and Structural Engineering, Kyushu University, Fukuoka, Japan.
[4]Principal, National Institute of Technology, Oita College Oita, Japan.
[5]Manager, Technical Center, Fuji P.S Corporation, Fukushima, Japan.
[6]Manager of Centre, Technical Center, Fuji P.S Corporation, Tokyo, Japan.

2018b). In addition, this paper is an extended and enhanced version of the work originally titled “Resistance against fatigue loading of precast PC deck slab with the improved loop joint.” reported at the ConMat’20 International Conference (Hatakeyama e*t al*. 2020).

2. Static loading test

A static loading test was conducted to understand the bending load-carrying performance of RC beams with the improved loop joint and to clarify the limit inclination angle, which maintains the minimum performance as a joint system for highways. The test was divided into Series A and Series B.

Series A is designed to evaluate the limit inclination angle. The internal diameter of the loop reinforcing bar was set to a constant value, and the inclination angle was varied as an experimental parameter. Notably, the effective height and the amount of reinforcing bars of each test specimen were not the same; hence, the flexural rigidity of each specimen was different. By contrast, Series B is designed to test the effectiveness of the angle of the loop joint and diameter of the reinforcing bar. In Series B, the deck slab thickness was set to a constant value of 220 mm in accordance with the minimum deck slab thickness according to the outline of bridge specifications (NEXCO 2017).

2.1 Details of loop joints

The design conditions for the static loading test were as follows: the cover and space of the reinforcing bar were approximately 40 mm, and the loop reinforcing bars were D19 (D: nominal diameter in mm) and D22, both of which are SD345 and arranged at intervals of 150 mm. The design compressive strength of the concrete was 50 N/mm^2. The allowable tensile stress of the reinforcing bar was controlled at 120 N/mm^2 with a margin of approximately 20 N/mm^2 to suppress the occurrence of harmful cracks and prevent the progress of concrete peeling based on Japanese Specifications for Highway Bridges (Japan Road Association 2012). For the loop reinforcing bar stress at the bending start point is controlled at 120 N/mm^2, the required bending diameter is approximately 80 mm ($< 5\varphi$) as calculated by Eq. (1):

$$dB = (1.4 + 2.8 \cdot \varphi / e) \cdot \varphi \cdot \sigma_e / \sigma_{ck} \geq 5\varphi \qquad (1)$$

where dB is the minimum internal diameter of the loop reinforcing bar (mm), φ is the diameter of the loop reinforcing bar (mm), e is the interval of the loop rebar (mm), σ_e is the reinforcing bar stress generated at the bending start point (N/mm^2), and σ_{ck} is the design compressive strength of concrete (N/mm^2).

Eq. (1) represents the minimum bending diameter of the loop reinforcing bar based on Leonhardt's equation (Leonhardt 1977). In this equation, the inclination angle of the improved loop joint is not specified. Therefore, the bending diameter for each series is set experimental.

Figure 3 shows setting the internal diameter of loop rebar. In Series A, the maximum inclination angle of the loop joint is set to 45°. The distance between the upper and lower sides of the reinforcing bar is set to be equivalent to the minimum bending diameter (= 81 mm) in the loop joint system, as shown in the side view of **Fig. 3(a)**. Therefore, the actual internal diameter of the loop reinforcing bar is 122 mm, and dB is greater than 5φ (= 95 mm).

In Series B, the deck slab thickness is set at 220 mm, and the cover concrete is set to a value greater than 40 mm. When the loop reinforcing bar of D22 with a minimum internal diameter of 111.5 mm was applied to the deck slab, the angle of the loop rebar was 62°. Then, another specimen with a loop reinforcing bar of D19, angle of 62°, and internal diameter of 114.5 mm was applied. In this series, all the specimens were set to the same effective depth of 169 mm.

The splice length at the joint was calculated assuming that the stress level of the reinforcing bar was 140 N/mm^2; in both Series A and B, the splice length was 250 mm to eliminate the influence of joint length and simplify the manufacturing of the specimens.

2.2 Specimen preparation

Table 1 lists the test specimens used in the static loading test, and **Table 2** lists the characteristic values of the specimens. Cross-sectional views of the joint position and bar arrangement of the test specimens are shown in

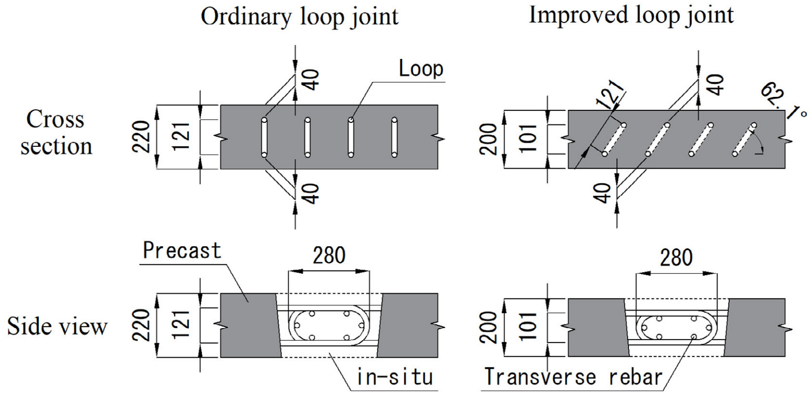

Fig. 2 Comparison of ordinary and improved loop joints.

Table 1 Test specimens for the static loading test.

Series	Specimens	Loop rebar diameter	Angle of loop joint	Internal diameter of loop rebar (mm)	Projection height of loop rebar (mm)	Slab thickness (mm)	Splice length (mm)
A	AN	D19	—	—	—	240	—
	A-19-90		90°	122.0	122	240	250
	A-19-75		75°	122.0	117	235	
	A-19-60		60°	122.0	103	221	
	A-19-45		45°	122.0	81	199	
B	B-19-90	D19	90°	99.0	99	220	250
	B-19-62	D19	62°	111.5	99	220	
	B-22-62	D22	62°	114.5	96	220	

Table 2 Material properties for the static loading test.

Series	Specimens	Concrete			Reinforcement bar	
		Compressive strength (N/mm^2)	Elastic modulus (kN/mm^2)	Tensile strength (N/mm^2)	Yield strength (N/mm^2)	Elastic modulus (kN/mm^2)
A	AN	68.3	28.6	4.15	368	202
	A-19-90	70.3	31.4	3.65		
	A-19-75	72.3	37.7	3.96		
	A-19-60	76.7	39.6	3.20		
	A-19-45	77.8	37.6	3.63		
B	B-19-90	72.3	37.7	3.96	376	195
	B-19-62	76.7	39.6	3.20	376	195
	B-22-62	77.8	37.6	3.63	380	200

Figs. 4 and **5**, respectively. All the specimens have a length of 3.0 m and width of 1.0 m. The joint width on the upper side is set to 330 mm, which is the same as that of the actual construction.

For Series A, the specimen AN, which is without a loop joint, has a part of cast-in-place in which two precast deck slabs are connected by continuous reinforcing bars. Test specimens other than AN were the ones in which the two precast deck slabs were joined by the loop joint. The ordinary loop joint was set to 90°, and the angle was decreased by 15°, such as 75°, 60°, and 45°. In specimens A-19-60 and A-19-45, the unreinforced part is generated at the end of the cross-section. Therefore, additional reinforcing bars are placed so that the reinforcing bar spacing is constant, as shown in **Figs. 4** (red framed part) and **5(c)** (colored steel bars).

2.3 Test setup

Figure 6 shows the loading outline, while **Fig. 7** shows an overall view of the test setup. The test is performed using four-point bending loading with a span length of 2800 mm and a loading span of 600 mm. The load is provided using a hydraulic jack and evaluated by the load cell. As shown in **Fig. 6**, the vertical displacement transducers (LVDTs) are placed just below the loading point and at mid-span. They are also placed at three

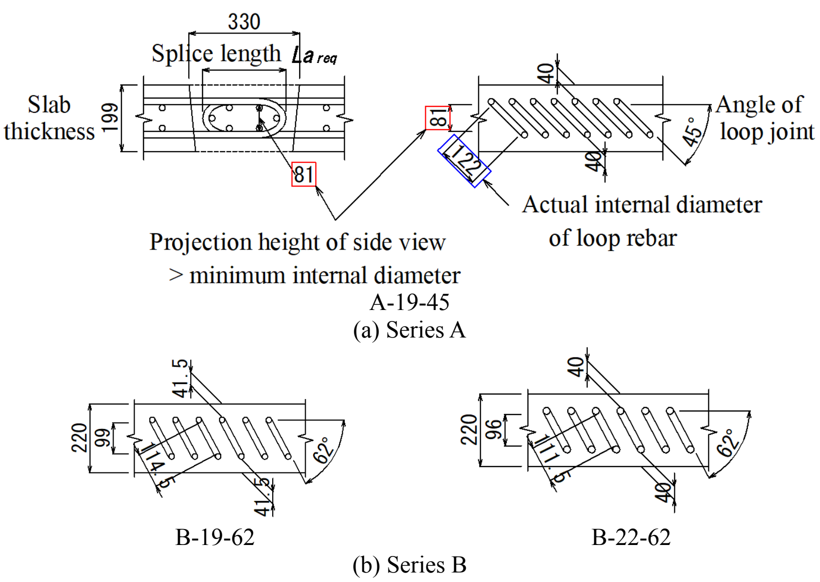

Fig. 3 Setting the internal diameter of loop rebar (unit: mm).

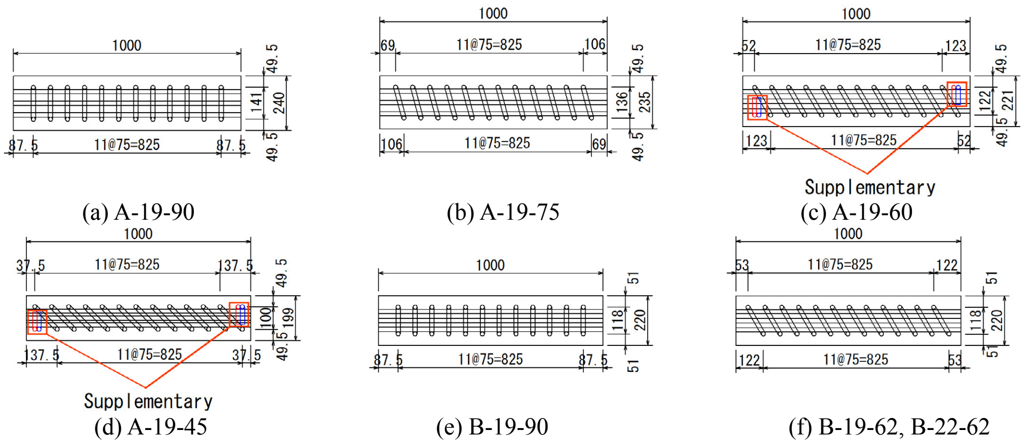

Fig. 4 Detail of joint section (unit: mm).

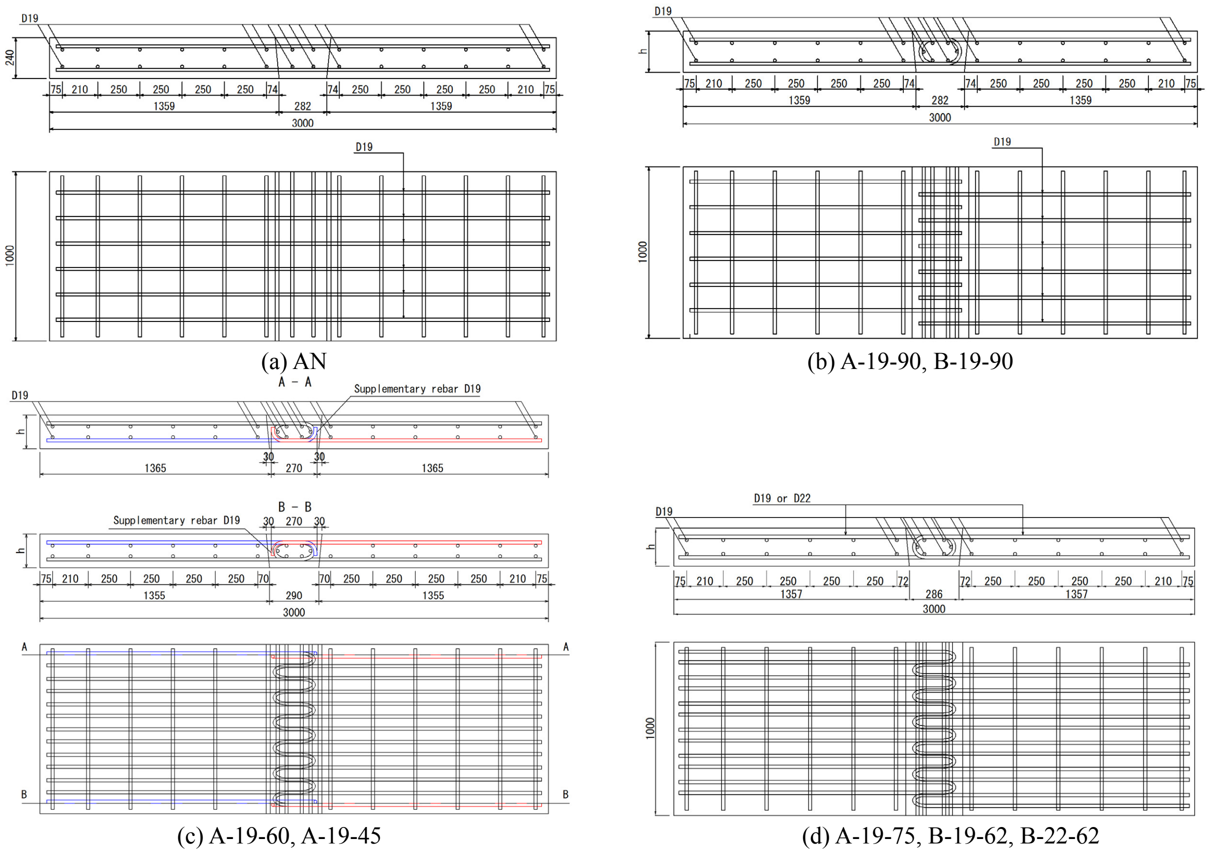

Fig. 5 Details of the specimens (unit: mm).

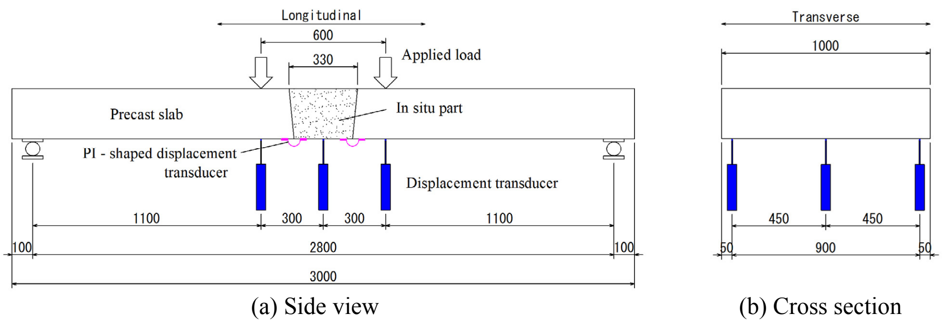

Fig. 6 Test setup.

Table 3 Results of theoretical calculation and experiment.

Specimens	Item	Joint opening	Cracking	Yielding of bar	Ultimate
AN	P_{cal} (kN)	–	80.0	203	248
	P_{exp} (kN)	25.0	65.0	191	290
	P_{exp} / P_{cal}	–	0.81	0.94	1.17
A-19-90	P_{cal} (kN)	–	69.8	203	250
	P_{exp} (kN)	10.0	90.0	203	297
	P_{exp} / P_{cal}	–	1.29	1.00	1.19
A-19-75	P_{cal} (kN)	–	71.5	198	245
	P_{exp} (kN)	40.0	55.0	190	266
	P_{exp} / P_{cal}	–	0.77	0.96	1.09
A-19-60	P_{cal} (kN)	–	50.9	211	260
	P_{exp} (kN)	25.0	60.0	210	299
	P_{exp} / P_{cal}	–	1.18	1.00	1.15
A-19-45	P_{cal} (kN)	–	47.1	186	233
	P_{exp} (kN)	25.0	55.0	171	253
	P_{exp} / P_{cal}	–	1.17	0.92	1.09
B-19-90	P_{cal} (kN)	–	71.5	184	226
	P_{exp} (kN)	33.0	60.0	171	263
	P_{exp} / P_{cal}	–	0.84	0.93	1.16
B-19-62	P_{cal} (kN)	–	71.6	185	228
	P_{exp} (kN)	25.0	40.0	160	267
	P_{exp} / P_{cal}	–	0.56	0.86	1.17
B-22-62	P_{cal} (kN)	–	70.8	245	283
	P_{exp} (kN)	30.0	55.0	231	321
	P_{exp} / P_{cal}	–	0.78	0.94	1.13

Note: P_{cal} : Theoretical calculation value, P_{exp} : Experimental value

points in the transverse direction. The amount of opening of the interface between the precast and cast-in-place parts is measured at the position shown in the figure using a PI-shaped displacement transducer. In addition, the strain of the reinforcing bars in the longitudinal axis direction near the joint is measured using strain gauges, and the strain gauges for concrete are attached only to the upper surface.

2.4 Results and discussion

(1) Deformation properties

The load versus mid-span deflection of each specimen is shown in **Fig. 8. Table 3** shows the results of the theoretical calculation and the experiment. The difference in

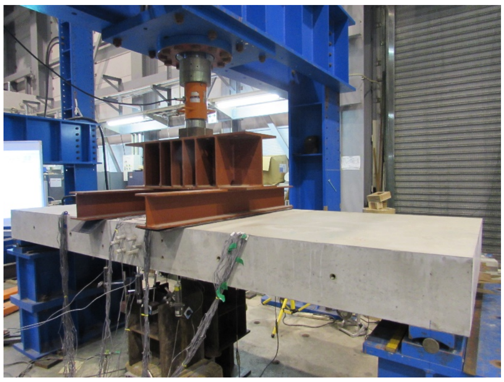

Fig. 7 Overall view of test setup.

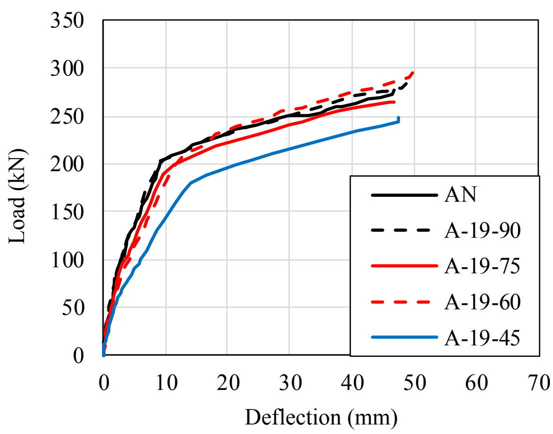

(a) Series A

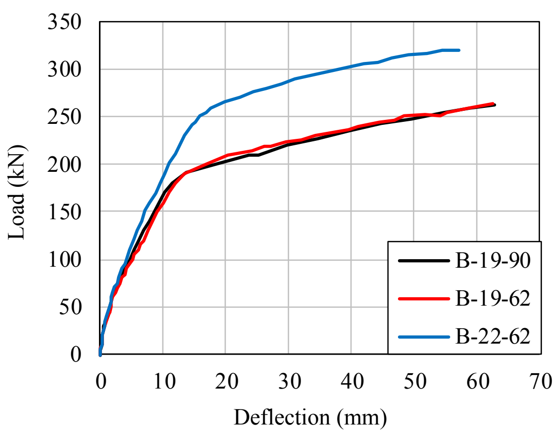

(b) Series B

Fig. 8 Load versus midspan deflection.

the three points of LVDTs in the transverse direction is less than 1 mm in every specimen; hence, the plotted values represent the average values of the three points. In addition, the cracking and yielding loads are calculated using the elastic theory of RC, and the ultimate load is calculated using the equivalent stress block. In all the specimens, the fracture was due to tensile failure, in which the upper surface of the concrete was crushed after the tensile reinforcing bar was yielded. A comparison of the specimens AN and A-19-90 of Series A indicated that the behavior of each specimen was the same under all loads. Hence, it can be said that the loop joint is an effective joint for reinforcing bar connections. It was observed that A-19-90 and A-19-75 exhibit similar behavior until cracks occur. However, A-19-75 shows a slightly larger displacement at the same load than A-19-90. This is because the effective depth of A-19-75 is 5 mm lower than that of A-19-90, and which is not due to the influence of the inclination. In A-19-60, the load-carrying behavior is the best of all specimens in Series A, as shown in **Table 3**. Although the effective depth of A-19-60 is lower than that of A-19-90, the amount of reinforcing bar of A-19-60 is greater than that of A-19-90. However, the deflection of A-19-45 is significantly larger than those of the other specimens. This is because the beam thickness of A-19-45 is the smallest among all the specimens, which causes a significant decrease in flexural rigidity. Focusing on the theoretical and experimental results for the ultimate load shown in **Table 3**, the results suggest that the loop joint inclined up to 45° still maintains the required performance as a joint system.

In Series B, the load-carrying behavior was the same as in Series A. From the test results, it was observed that B-19-90 and B-19-62 exhibited similar behavior in every load step; thus, it can be inferred that the inclination of the loop reinforcing bar does not affect the structure of the joint until 62°. Additionally, the behavior of B-22-62 is similar to the other specimens, and the experimental and calculated values are approximately the same. However, for the same effective depth of the loop reinforcing bar, the influence of the inclination of the loop rebar was not confirmed.

(2) Crack properties

Figure 9 shows the joint opening versus load increment. The AN data could not be recorded up to 100 kN; hence, it is not shown in **Figs. 9(a)** and **9(c)**. As shown in **Figs. 9(a)** and **9(b)**, all the test specimens have the same amount of opening before the rebar yields and behave the same as AN. Even after the yielding of the reinforcing bar, there is no significant progress in the opening and no deterioration in the bending performance. **Figures 9(c)** and **9(d)** highlight the navy-blue dashed frame portion of **Figs. 9(a)** and **9(b)** respectively. The inflection point of the amount of opening at the initial stage of loading is different for each test specimen. This is due to the difference in the deck slab thickness. The marks ◇ in the figures show the loads at which the stress of the tensile reinforcing bar reaches 100 N/mm^2. According to the Specifications for Highway Bridges (Japan Road Association 2012), it is described that the crack width should be less than 0.2 mm when the tensile reinforcing bar stress is 100 N/mm^2. In this test, the amount of joint

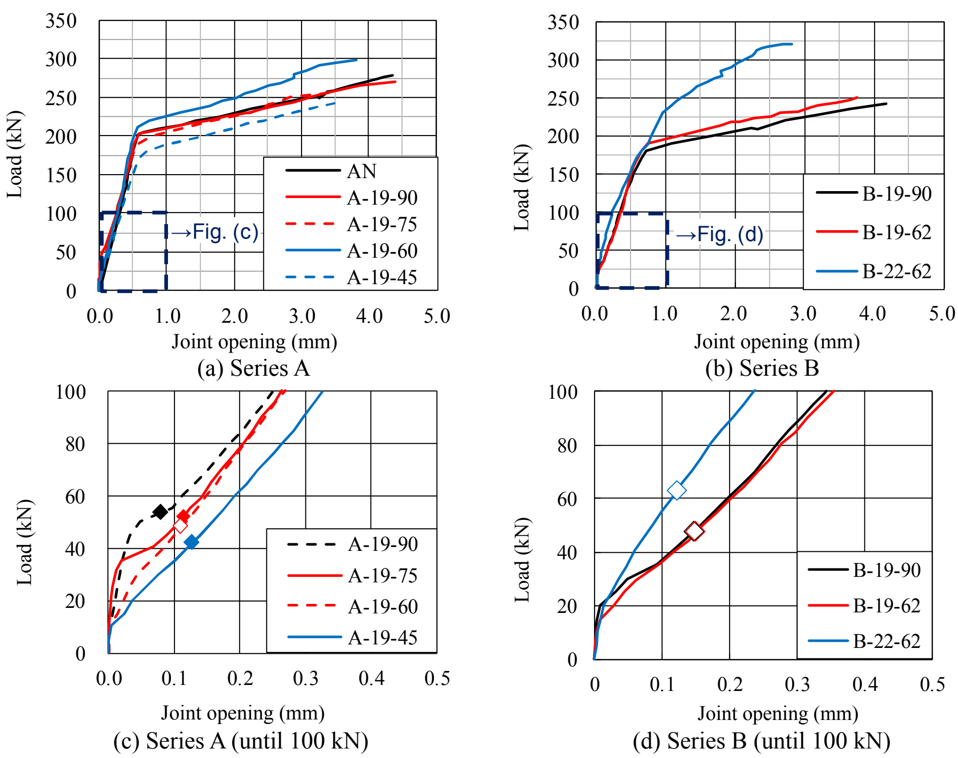

Fig. 9 Load versus joint opening.

opening is approximately 0.2 mm even under the design load; therefore, it is considered that the required durability is satisfied.

Figure 10 shows the crack patterns of each specimen after the loading test. As shown in the figure, there is no significant difference in the crack pattern, crack interval, and crack width among all the test specimens with loop joints and AN, even if the angle is changed from 90° to 45°.

3. Wheel moving load test

3.1 Specimen preparation

Figure 11 shows the specimen dimensions and positions of the displacement transducers. **Figure 12** shows the cross-section of the joint position of the specimen. The specimen consists of three parts: two precast PC slabs with improved loop joints and in situ concrete. For each slab, pre-stress is introduced in the direction perpendicular to the longitudinal axis (y-axis) to limit the tensile stress within 2 N/mm^2 at the bottom edge of the slab against its bending action under the live load. The parts are connected to form a single one-way PC slab by casting concrete between them. The dimension of the specimen is 4500 × 2800 mm with a thickness of 220 mm at the center of the span. Loop rebars (D19) are arranged at intervals of 150 mm. The inclination angle of the loop rebar is set to 62° to reduce the deck slab thickness from 240 mm to 220 mm when using the D22 loop rebar, as described in the static loading test Series B. The required deck slab thickness is the sum of the required internal bending diameter of the loop rebar, twice the cover thickness, and the reinforcing bar diameter. The required internal bending diameter *dB*(mm) is calculated using Eq. (1), and the cover thickness is 40 mm. The material properties are listed in **Table 4**.

3.2 Test setup

(1) Wheel moving load test machine

The test was conducted using a wheel moving load test machine, as shown in **Fig. 13**. The iron wheel of the test machine has a diameter of 0.7 m and a width of 0.5 m. It operates in reciprocating motion. The maximum load during running of the iron wheel is 490 kN. The maximum reciprocation speed is 15 reciprocations per minute, and the test is performed at a speed of 10–15 reciprocations per minute.

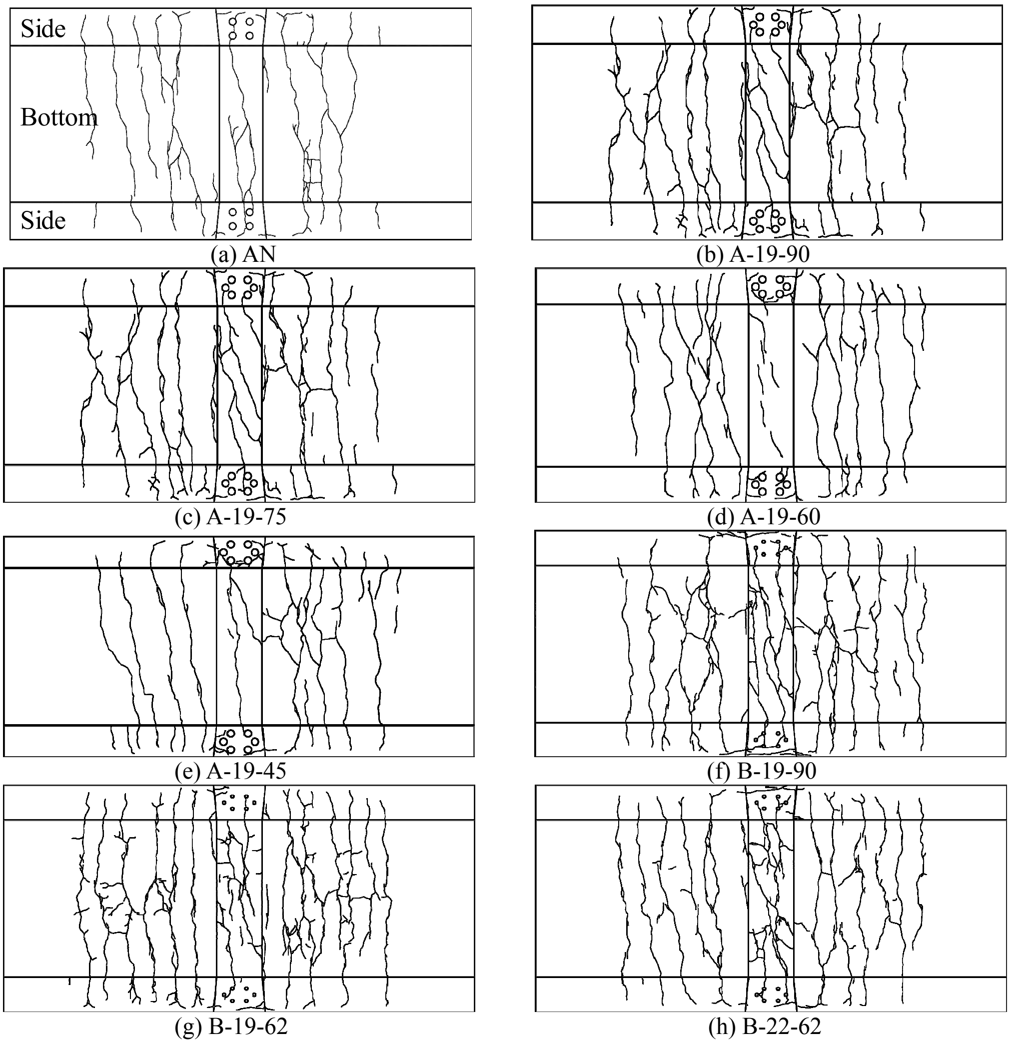

Fig. 10 Crack pattern after loading test.

Table 4 Material property values for the wheel moving load test (unit: N/mm^2).

Material		f_c'	E_c	f_y	f_u	E_s	Remark
Concrete	Precast deck slab	76.8	39 200	—	—	—	79 days after placing
	Cast in place	60.3	33 700	—	—	—	39 days after placing (with expansive additive)
Reinforcing bar	D13, D19	—	—	400	550	200 000	Epoxy resin coating
PC steel strand	1S15.2	—	—	1812	1962	191 000	

Note: f_c' : compressive strength, E_c , E_s : Young's modulus, f_u : tensile strength, f_y : yield strength

(2) Conditions and instrumentation

The support requirement is a simple support with a span length of 2500 mm, and the wheel repeatedly travels within the range of 500 mm in width and 3000 mm in length, as shown by the red dashed line in **Fig. 11**. **Figure 14** shows the load-step diagram. In this test, 250 kN × 100 000 passages are conducted to investigate the durability equivalent to 100 years (Nagao and Hirose 2012). Subsequently, a water-filling test is conducted to check the water leakage from the joint between the precast part and the in situ part. The water-filling test setup is shown in **Fig. 15**. In the water-filling test, the water depth is maintained at 10 mm, and the water is allowed to flow for 6 h. After the test is completed, water is emptied, and the load is increased by 50 kN every 40 000 passages to investigate the fatigue fracture properties of the specimen, as shown in **Fig. 14**. The load is increased to 490 kN, which is the maximum load of the machine. The total number of loadings at each loading stage is 460 000. The number of converted loading times N_{eq} running under this condition is calculated using Eq. (2) as:

$$N_{eq} = \sum \left(\frac{P_i}{P_0} \right)^m \times N_i \quad (2)$$

where P_0 is the basic axle load (= 157 kN), P_i is the wheel load (kN), m is the absolute value of the reciprocal of S-N curve slope (= 12.76) proposed by Matsui (2007), the deck slab surface condition is dry, and N_i is the number of loadings at the wheel load P_i.

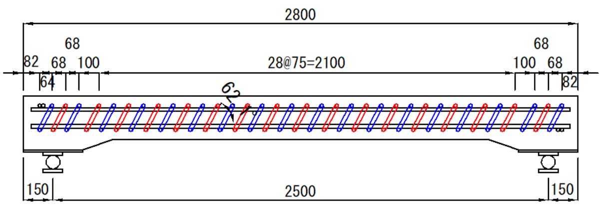

Fig. 12 Cross-section of joint position (unit: mm).

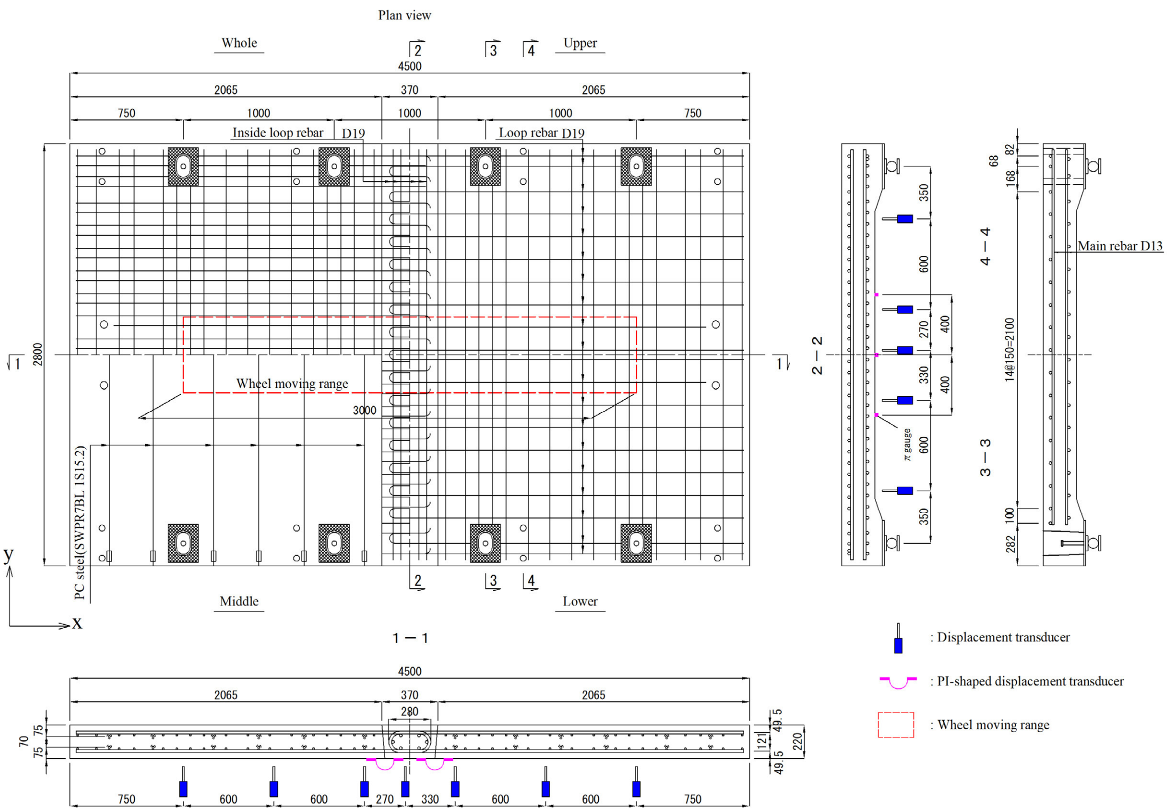

Fig. 11 Specimen dimensions and arrangement of displacement transducers (unit: mm).

Static loading was performed in the center of the deck slab after a predetermined number of loadings. During the loading test, the deflection of the slab, strain of the reinforcing bar, and amount of joint opening at the interface between the precast and in situ parts were measured. The deflection of the slab was measured using vertical displacement transducers (LVDTs), and the joint opening was measured using PI-shaped displacement transducers (PI gauge). The arrangement of the LVDT and PI gauges is shown in **Fig. 11**.

3.3 Results and discussion

(1) Deflection at mid-span

Figure 16 shows the changes in deflection at the center of the slab. **Figure 16(a)** shows the details of 250 kN × 100 000 passages, which is equivalent to 100 years, and **Fig. 16(b)** shows the results of the total load steps. The live load deflection δ_{live} is calculated using Eq. (3) as:

$$\delta_{lives} = \delta_{total} - \delta_{residual} \quad (3)$$

where δ_{total} is the total deflection measured by the LVDT at the maximum load in each loading stage, and $\delta_{residual}$ is the residual deflection measured during unloading. The total and residual deflections gradually increased with an increase in loading. However, the deflection after the loading of 490 kN tended to increase more than before. By contrast, the live load deflection was almost constant at all loading stages. A similar tendency was observed for the other LVDTs, and no drastic change was observed in the deflection due to the loop joint.

(2) Deflection distribution

Figure 17 shows the deflection distribution in the live load. **Figure 17(a)** shows the y-axis direction (between the slab supports), and **Fig. 17(b)** shows the x-axis direction (perpendicular to the slab supports). The data shown in the diagram are that of the live load deflections taken at the final loading in each loading stage. It can be confirmed that the deflection of the live load increases at

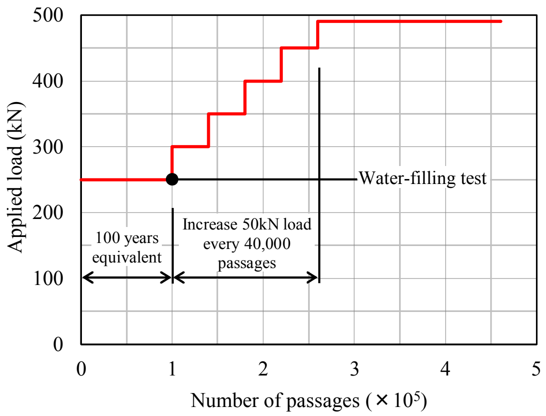

Fig. 14 Load step diagram.

Fig. 13 Wheel moving load test machine.

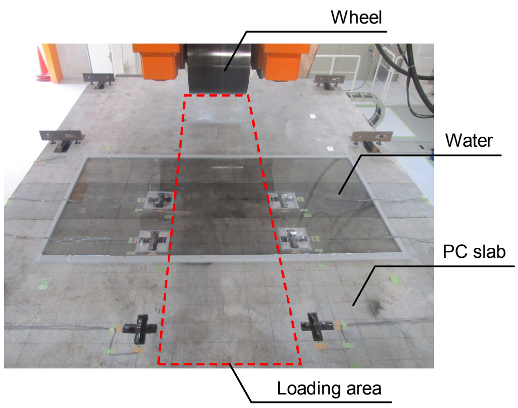

Fig. 15 Water filling test.

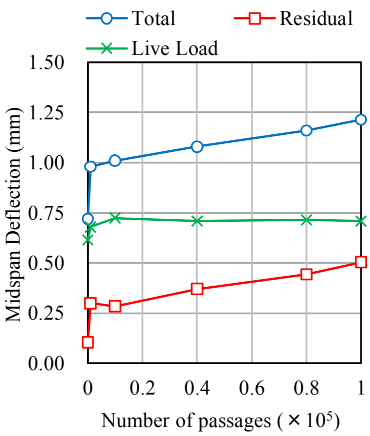

(a) Until 100 000 passages (250 kN)

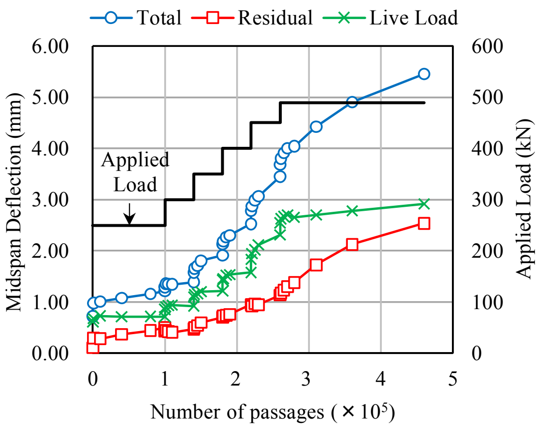

(b) Total

Fig. 16 Changes of mid-span deflection.

any measurement position as the applied load increases, and the deflection difference between the steps increases as the loading increases. In **Fig. 17**, when comparing the left and right deflections at the span center, it was confirmed that the values were symmetrical at all loading stages. In addition, it is considered that there is no difference in the flexural behavior in both the x and y-axis directions, even if the loop reinforcement is placed at an angle of 62°.

(3) Joint opening between the PC deck slab and in situ part

Figure 18 shows the changes in the joint opening between the PC deck slab and in situ part. The figure shows the values below the loading point, which is the largest value among all six locations. The legend color is the same as that shown in **Fig. 16**. As shown in **Fig. 18(b)**, the joint opening at each load stage fluctuated and did not show a constant value, unlike in the case of deflection. It can be inferred that a small level difference in the vertical direction occurred during each run owing to the impact of the wheel load. However, the fatigue durability of 250 kN × 100 000 passages that is equivalent to 100 years in **Fig. 18(a)** resulted in the largest joint opening of 0.07 mm, which was very small. No water leakage from the joints on the lower surface was observed in the water-filling test after 250 kN × 100 000 passages. Therefore, it is considered that the proposed loop joint has fatigue durability equivalent to 100 years.

(4) Crack progress

Figure 19 shows the progress in the crack for different loads. Up to 250 kN, cracks in the y-axis direction occur at the joint interface and precast parts. After that, cracks do not occur in the in situ sections in the x-axis direction. Therefore, it is considered that the fatigue durability of the in situ part with the inclined loop joints is equal to or better than that of the ordinary joint of the PC deck slab. The punching shear failure due to fatigue loading did not occur even after loading 490 kN × 200 000 passages; therefore, the improved loop joint is considered to have sufficient fatigue durability.

4. Conclusions

In this study, we conducted a static loading test and a wheel moving load test to clarify the performance of the improved loop connection as the joint structure of precast concrete slabs. The following conclusions were derived from the test results.

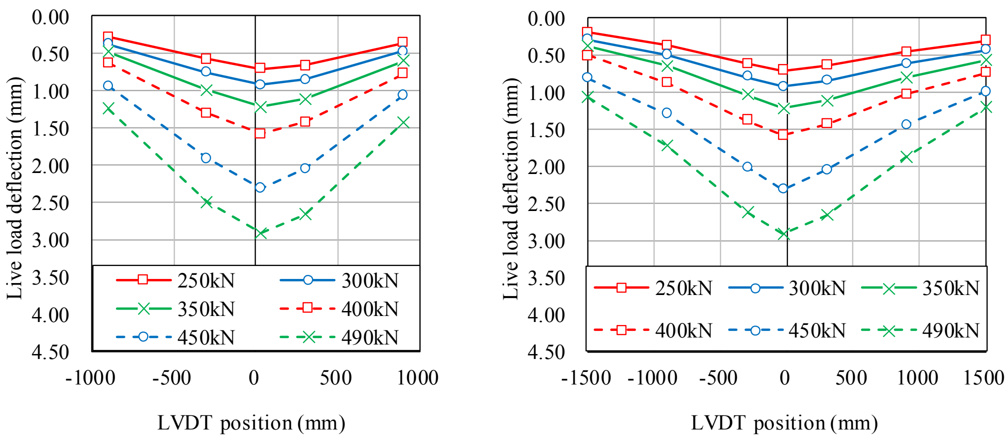

(a) y-axis direction (b) x-axis direction

Fig. 17 Live load deflection distribution.

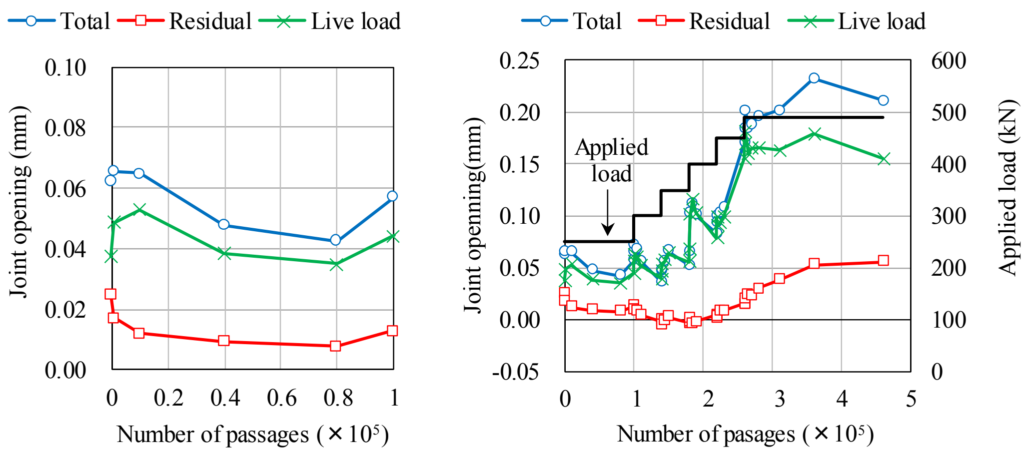

(a) Until 100 000 passages (250 kN) (b) Total

Fig. 18 Changes of joint opening between deck slab and in-situ part.

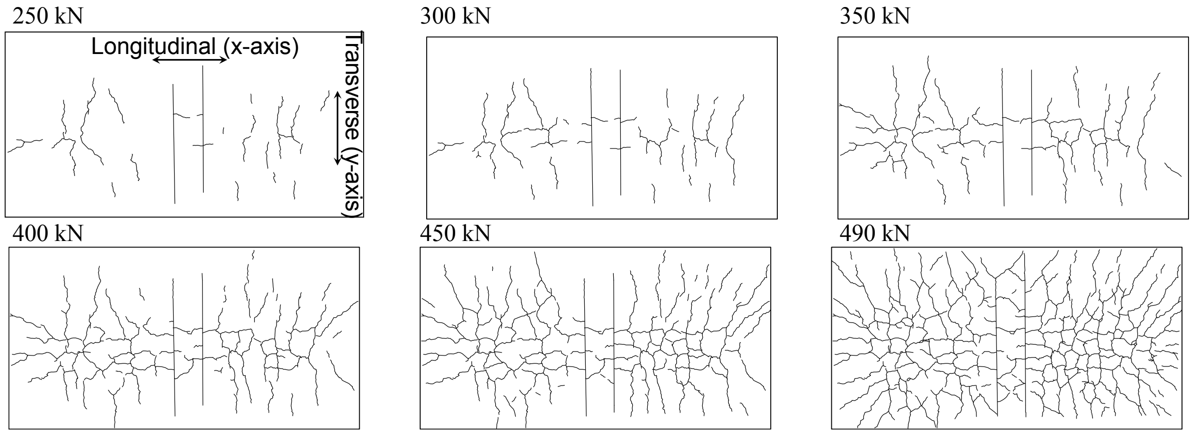

Fig. 19 Crack progress.

From the static loading test,

1) The improved loop connection was considered ideal to work as the joint structure of precast concrete even if inclined up to 45° (Series A).
2) The inclination of the loop reinforcing bar did not affect the load-carrying behavior (Series B).
3) The design value of the yielding and ultimate loads was calculated using the elasticity theory and equivalent stress block of the RC member (Series A and B).

From the wheel moving load test,

4) No sudden increment in vertical deflection or no joint opening was observed at the designated load step (250 kN × 100 000 passages), which is equivalent to 100 years for actual bridge structures.
5) There was no water leakage from the bottom surface of the deck slab during the water-filling test.
6) The cracks did not occur rapidly in the in situ part, and the final cracking pattern was bidirectional that is similar to the general crack progress. Therefore, no harmful effect of the inclined arrangement of the loop reinforcing bars was confirmed.
7) Even after the loading of 490 kN × 200 000 times, no punching shear failure due to fatigue loading occurred.
8) Based on the above results, it is considered that the improved loop joint has sufficient fatigue durability when the loop rebar angle is in the range of 62° to 90°.

Acknowledgments

The authors express their gratitude to Nippon Expressway Research Institute Company Limited for providing advice on the test method and for valuable discussions.

References

Hatakeyama, S., Hino, S., Masaki, M. and Sato, Y., (2018a). "Experimental study on bending load capacity of slab with slanted loop joints in-situ cast concrete." *Proceedings of the Japan Concrete Institute*, 40, 589-594. (in Japanese)

Hatakeyama, S., Sato, Y., Masaki, M. and Hino, S., (2018b). "Fundamental study on application of improved loop joint structure of precast PC slab." *Proceedings of the 28th Symposium on Developments in Prestressed Concrete*, Matsuyama Japan. Tokyo: Japan Prestressed Concrete Institute, 379-382. (in Japanese)

Hatakeyama, S., Hino, S., Hamada, H., Sagawa, Y., Sato, Y., Kawabe, S. and Masaki, M., (2020). "Resistance against fatigue loading of precast PC deck slab with the improved loop joint." *6th International Conference on Construction Materials*, 796-805.

Henrik, B. J. and Linh, C. H., (2013). "Tests and limit analysis of loop connections between precast concrete elements loaded in tension." *Engineering Structures* 52, 558-569.

Japan Road Association, (2012). "*Specifications for highway bridges, Part 3 Concrete bridges.*" Japan Road Association. (in Japanese)

Leonhardt, F., (1977). "*Vorlesungen Über Massivbau, vol.3.*" Tokyo: Kajima Institute Publishing Co. Ltd. (in Japanese)

Matsui, S., (2007). "*Road bridge decks: design, construction, and maintenance.*" Tokyo: Morikita Publishing. (in Japanese)

Nagao, C. and Hirose, T., (2017). "The fatigue durability checking test of joints between precast PC decks." *Proceedings of the 27th Symposium on Developments in Prestressed Concrete*, Kobe Japan. Tokyo: Japan Prestressed Concrete Institute, 189-192. (in Japanese)

NEXCO, (2017). "*Expressway standard technical specifications by NEXCO – Outline of bridge specifications Vol.2.*" Japan: Nippon Expressway Research Institute Co., Ltd. (in Japanese)

Ong, K. C. G., Hao, J. B. and Paramasivam, P., (2006). "Flexural behavior of precast joints with horizontal loop connections." *ACI Structural Journal*, 103(5), 664-671.

Ryu, H. K., Kim, Y. J. and Chang, S. P., (2007). "Experimental study on static and fatigue strength of loop joints." *Engineering Structures*, 29, 145-162.